International Journal of Railway Research, Vol. 2, No. 2, (2015), 37-47

Iran University of Science and Technology

International Journal of

Railway Research

ISSN: 2423-3838

Modelling and Simulation of Electric Trains in the Presence of Ultra-capacitor as Energy Storage

Mohsen Maaleky [1*], Bijan Moaveni [2]

[1]Electric Railway Expert

[2]Associate Professor of Control Engineering, Iran University of Science and Technology, Tehran, Iran

ARTICLE INFO

Article history:
Received: 5.03.2015
Accepted: 18.05.2015
Published: 30.06.2015

Keywords:
Hybrid Electric Train
Energy saving
Optimization
Simulation
Ultra-capacitor

A B S T R A C T

When a vehicle brakes, energy is released. To date, considerable amount of the braking energy is lost in hot air. The challenging alternative is to store the braking energy and use it during acceleration or autonomous operation of the vehicle. As a consideration of progress in hybrid and energy storage technology in heavy transportation a simple and precise model of train equipped with ultra-capacitor modules as energy storage system is modeled and simulated in MATLAB/Simulink environment. The simulation results show that its technology is mature enough to be used in railway transportation and it has many advantages over the customary batteries.

1. Introduction

Today, energy consumption and reducing the air pollution are becoming more and more important issues in the worldwide scale as well as the transportation industry [1, 2]. In transportation industry, the hybrid vehicles that use recovered energy are proposed to deal with these important problems [3]. Nowadays, there are lots of small and large vehicles that use variety of hybrid configuration to reduce fuel consumption and environmental emissions. It seems that hybrid technology is mature enough to be used in mass transportation industry [2]. Moreover, with respect to development in technology of producing ultra-capacitors and super-capacitors, it seems that the hybrid vehicles and corresponding transportation are feasible to be discussed in more details [4]. There are clear benefits of having an energy storage device allowing start-stop operation and the re-use of energy absorbed during the braking process. Also, in case of trams and trains primary energy demand can be reduced significantly, allowing longer, more or higher performance vehicles on an existing track [5].

One of the energy storage devices is rechargeable batteries, but in fact they have some serious limitations for this kind of application. Batteries are heavy, large in size, have a limited charging rate and potentially high maintenance costs [4]. They also can suffer degraded performance at low temperatures [6]. It is believed that rapid transients in power demand will be better handled by the use of high power density ultra-capacitors [6]. Ultra-capacitors, or double-layer capacitors, provide high charge acceptance, high-efficiency, cycle stability and excellent low-temperature performance [6]. The difference between super-capacitors and ultra-capacitors is only in their construction. Super-capacitors use porous carbon electrodes with high surface areas and do not involve an

*Corresponding author
Email address: Mohsenmaaleky@gmail.com

electrochemical reaction (Electrostatic), while ultra-capacitors store their energy electrochemically in a polarized liquid layer which occurs at the interface between the electrolyte and electrode (Electrolytic) [4]. Many times, the terms super-capacitor and ultra-capacitor are used interchangeably, however it is important to note that these are two distinct technologies with somewhat different operating characteristics [4].

There are many researches about hybrid vehicles based on the different structures with the use of battery and some with ultra-capacitors in the literature [7, 8, 9]. But, there are little researches about heavy vehicles as railcars [10]. As a practical sample, "SITRAS" that is developed by Siemens to be used in several cities such as Madrid in Spain and Cologne in Germany [5]. SITRAS is an innovative energy storage system that is also designed to recover braking energy. The system is not placed on the vehicle, but it uses ultra-capacitor banks to recover braking energy and maintain the voltage, stable. It provides a peak power capacity of one megawatts. But the weakness is its radius of operation that it is just about 3 kilometers [5]. Another attractive technology is MITRAC technology by Bombardier corp. The Bombardier MITRAC energy saver works by charging storage devices with electrical energy released when braking. The system is based on high-performance double layer capacitor technology which allows frequent starting and braking. The stored energy can be used in many ways resulting in various benefits [11].

There are lots of researches and articles about modeling and simulation of small and heavy cars but not much reliable and precise models for electric hybrid train [10]. In this paper, the modeling and simulation of Tehran metro railcar equipped with a Maxwell ultra-capacitor module as energy storage is introduced. In the first step, a reliable and practical model of a hybrid train that can be used for next researches is established. In the next step, the effect of using ultra-capacitor inside train to recover the energy is studied. Table 1 presents the characteristics of the simulated system.

2. Model Based Design of Electric Train System

There are many software and toolboxes for modeling and simulation of conventional vehicles, such as Autonomie, SimDriveline, SIMPLEV, V-Elph, Saber, Simulink and Advisor [7, 12, 13, 14]. But, none of them can be used to model the hybrid electrical train [10].

Table 1. Characteristics of the simulated system

Weight per axle	13.7325	Ton
Davis coefficients	A	11 m^2
	B	20.1168
	C	$6.7947 \cdot 10^{-5}$
Traction system	DC machine	132 *KW*
Max. acceleration	0.6	m / s^2
Max. deceleration	0.7	m / s^2
Gear ratio	91:15	-
Wheel radius	0.430	*m*
Voltage	300 – 500	*volts*
Max. current	400	*A*
Energy storage weight	363	*Kg*
Energy storage capacity (stored energy)	860.2	*Ah*
Energy storage max. power	3800	*W / Kg*

Here, a model based design to model a hybrid electrical train is presented. It is regarding the Advisor approach, due to its simplicity and reliability [7, 15, 16]. The concept of the approach is shown in Figure 1. In most basic form, "model based system design" is a method which uses the models of components to describe the specifications, operations and performance of the corresponding system [17]. Instead of listing specification in a text document, a model is used that implements the specifications, operation, and performance of components [17]. It is worth noting that, in this paper, simulation of the hybrid train is performed in MATLAB/Simulink environment

based on the ideas which were introduced in Advisor. It is clear that Advisor has so many details that don't need to be included in this simulation. As it is shown in Figure 2, and regarding the backward/ forward approach introduced in Advisor, arrows from left to right correspond to the related backward facing that illustrate forward facing connection.

$$F = m \cdot a \tag{1}$$

Where m is total mass of the vehicle in kilograms, a is its acceleration in meter per second squared and F is required tractive force to accelerate the train in Newton. In addition to main pulling or pushing force of the train, there are three resistive forces that influence the motion of the vehicle.

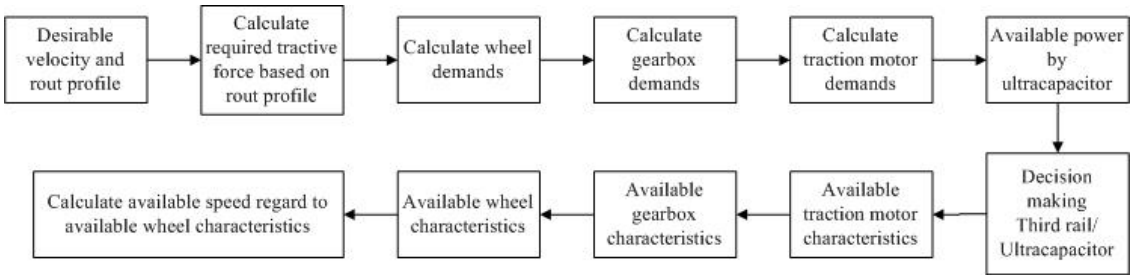

Figure 1. Backward/ Forward approach flowchart

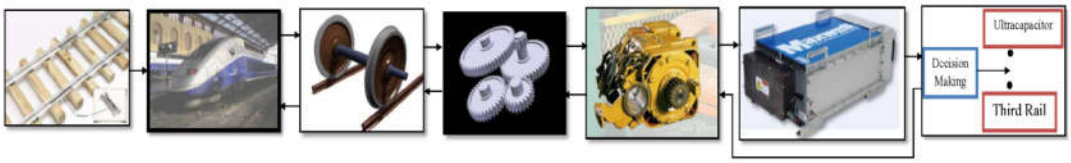

Figure 2. Block diagram of complete system

2.1. Drive Cycle Modeling

The first block of the system in Figure 1, is drive cycle. It represents the desired velocity; grade and curve profiles of route at each time of the cycle. Obviously, it can be modeled by a matrix that its first column is time and the second column is the corresponding desired velocity at related time. By integration of velocity, distance is obtained. So, by using the grade and curve profiles of the route, the grade versus distance and curve versus distance lookup tables as can be provided as is shown in Figure 3.

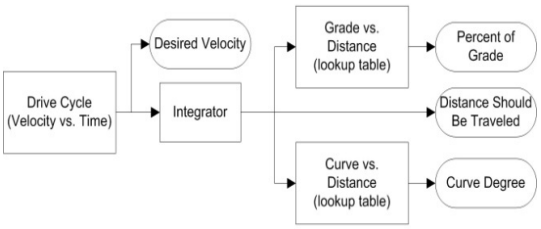

Figure 3. Drive cycle block diagram

2.2. Modeling the Longitudinal Dynamics

The main relation that governs the longitudinal dynamic of any vehicle is the Newton's second law of motion in Equation (1):

A set of resistance forces can be modeled by using the Davis formula [18]:

$$R_D = (5.78266 \cdot M \cdot n + 128.997 \cdot n) + (B \cdot M \cdot n) \cdot v + C \cdot A \cdot v^2 \tag{2}$$

Where, A, B, and C are the coefficients that depend on the type of the trains. The values of these coefficients that are used in this research are illustrated in Table 1. A schematic for the grade forces on a train is presented in Figure 4.

Also, in Equation (2) v is train velocity, and R_D is the total resistance of train in Newton [19]. Another part of the resistive forces is the grade resistance which can be described as in Equation (3):

$$R_g = 88.964 \cdot n \cdot M \cdot G \quad (3)$$

Where, R_g is grade resistance in Newton and G is percentage of the grade. It is important to note that, R_g has a positive sign in downgrades and a negative sign in upgrades due to the backward facing approach. The last part of the resistive forces is the curve resistance (R_c) from friction of wheel flanges against rails as a train goes around a curve. Railroad curve resistance is 3.5587 Newton per Ton of car per degree of curvature. In other word, a 100 ton car on a 2 degree curve has a resistive force equal to 711.7154 Newton. So, to compute the curve resistance the Degree of Curvature should be determined as follows [18, 20]:

$$\text{Degree of Curvature} = \frac{1146}{\text{Curvature Radius [m]}} \quad (4)$$

So, the total required tractive force of a train can be calculated as follows:

$$F_T = F + R_D + R_g + R_C \quad (5)$$

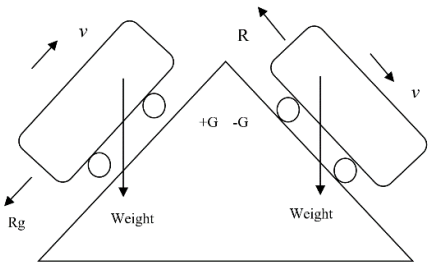

Figure 4. Corresponding grade forces on train

The details of the train dynamic block diagram are illustrated in Figure 5. The input of this block is the desired velocity and the output is the corresponding required traction force and speed of the train. In this block, the required traction force is computed based on the Equations (1)-(5).

In the bottom part of Figure 5, there is another input (Available Tractive Force) that is related to the available speed and traction force at the end of forward facing approach. Here, the available tractive force solves as a quadratic function to calculate the previous velocity, using the equations used in backward facing approach. It means that at the end of each time step, the velocity of the train is obtained and by this the difference between the desired and the available speed can be calculated. By integrating of the speed in the elapsed time the traveled distance can be calculated.

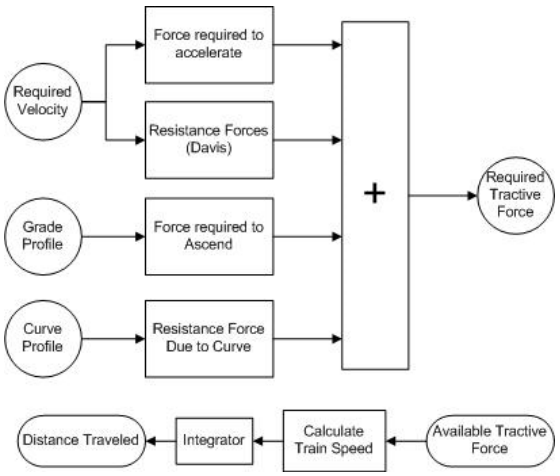

Figure 5. Train dynamics block diagram

2.3. Wheel Modeling

Another important part of the system modeling is the wheels dynamic. The wheels are modeled by using a simple model as mentioned in Figure and by using Equation (6).

$$J\dot{\omega} = T - r \cdot F_T \quad (6)$$

where J and r denote the inertia and the radius of the wheel, respectively. Also, T describes the driving or braking torque and ω is the angular velocity of the wheel. The steady state wheel forces and torques are generated as functions of the slip-augmented rotational speed. The longitudinal force F_T can be described as a function of the longitudinal slip, s_x. The longitudinal slip is defined as in Equation (7) and Figure 6 shows the relation between F_T and s_x [21]:

$$s_x = \frac{v - r\omega}{v} \quad (7)$$

The slip is not directly calculated by using Equation (7). It is just assumed that the slip is controlled between the reasonable values and by dividing tractive force by the force on the wheel the coefficient of friction (μ) will be obtained. Regarding Figure 7, the slip value will be gained and the angular velocity based on Equation (7) is calculated. In the wheel block of Figure 2, the force and the vehicle longitudinal velocity are the input. By using the weight on the wheel and a lookup table the loss of the wheel is attained. The effect of the inertia is calculated by using Equation (8). The wheel loss and the effect of the inertia are added to the required torque in backward facing approach. In forward facing they will be declined.

$$\text{Effect of Inertia} = \left(\frac{\omega - \omega_{previous}}{t - t_{previous}}\right) \cdot r \quad (8)$$

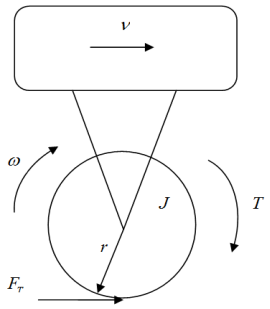

Figure 6. Simple chassis/wheel model

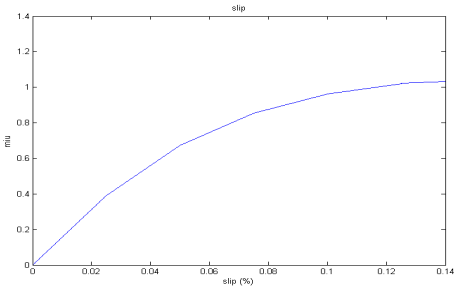

Figure 7. Longitudinal slip characteristics of train

The detail of the wheel model Block is shown in Figure 8. A brake controller interface is placed in the block to simulate the friction braking when the vehicle velocity is less than 10 Km/h. As mentioned in [10] in velocities less than 10 km/h, the motor rotational speed is not enough to generate the minimum charging power of the ultra-capacitor, but based on Tehran metro documents the minimum speed that can be used for the dynamic braking is 30 km/h. In speeds below this value, the friction braking takes over for most of the braking.

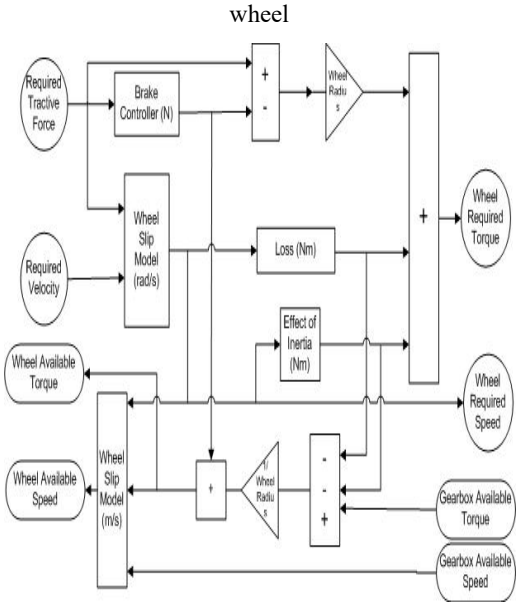

Figure 8. Wheel model block diagram

2.4. Gearbox Modeling

The gearbox is modeled with a simple form. Generally it is described in the equation below:

$$\pm G_{FB} = \frac{\omega_B}{\omega_F} = \frac{T_F}{T_B} \quad (9)$$

where G_{FB} is gear ratio; and indices F and B denote follower and base, respectively. Also, ± denotes rolling direction of gear and shaft. As mentioned before in each block the inertia and loss of the corresponding block is computed and added to results. The subsystem "Effect of Inertia" in Figure 9 is related to gearbox inertia. Here the loss of gearbox is ignored.

2.5. Traction Motor Modeling

As mentioned in many references like [22] and [23], in large and complex systems such as vehicles, employing the efficiency maps of the motor is an appropriate way to model the traction motor. Using the efficiency maps, motor is modeled as a black box that according to the applied required speed and torque as inputs

serves a known output like amount of Kilowatts that is needed to be supplied. The efficiency map of DC machine which is used in the simulations is shown in Figure 10.

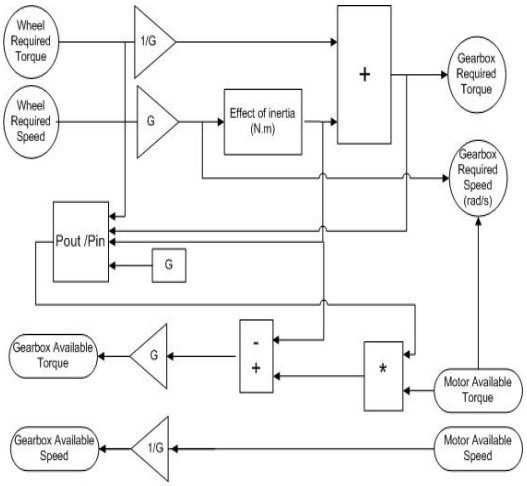

Figure 9. Gearbox model block diagram

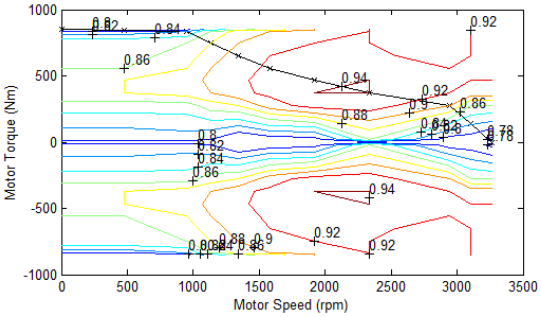

Figure 10. Efficiency map of a DC traction machine

Generally, the efficiency map is the torque/speed curve of a certain electric machine that is special for it. The torque/ speed curve is mapped by efficiency map of the machine in each point. Using this map, the power loss of the machine can be calculated and be added to the output power of the machine ($P_{out} = T \cdot \omega$), so the required input power is easily calculable. The schematic diagram of the traction motor is shown in Figure 11.

2.6. Ultra-capacitor and Bus

2.6.1. Ultra-capacitor specifications and benefits

Heavy transportation vehicles place particular demands on energy storage devices. They must be very robust and reliable, with a long lifetime and low maintenance requirements. They must be able to operate efficiently under harsh conditions, and they must be able to

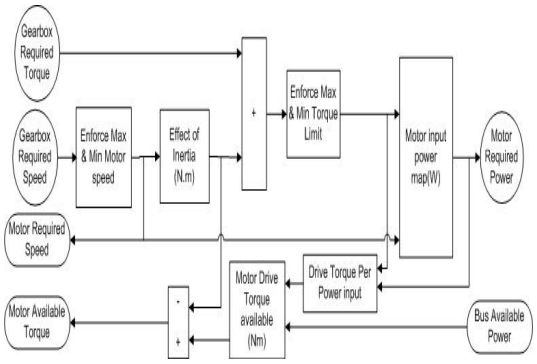

Figure 11. Motor and controller model block diagram

deliver high peak currents. They must also be able to work on a high duty cycle and cope with frequent deep discharging. Finally, they must be straightforward to integrate into a vehicle design [3]. Maxwell Technologies has addressed these issues with its HTM BOOSTCAP ultra-capacitor module for ultra-capacitor-based braking energy recuperation and torque assist systems in transportation applications [3]. By operating at 125V, the new module can store more energy per unit volume, deliver more power per unit volume and weight and last longer than any other commercially available ultra-capacitor solution [3]. A key factor in the energy storage system is thermal management. With efficient cooling, higher continuous currents are possible without compromising reliability.

The dimensions and design of the 125V module were chosen for best efficiency and cooling behavior when operated at high currents, up to 150A continuous and 750A peak. This compares to a maximum continuous current of 90A with Maxwell's 48V ultra-capacitor module, an increase up to 70%. This means that a much higher charge/discharge power can be delivered [3].

The module design ensures that there is only a 3°C temperature rise above ambient temperature at the maximum continuous current. The layout of the module results in a very stable temperature distribution over all cells in the module, which results in greater reliability and longer life [3].

The HTM module is designed to perform reliable work through one million or more charge/discharge cycles, which equates to

150,000 hours or more than 15 years of operational life. It is undergoing extensive testing against rigorous transportation industry standards [3].

Proprietary material science and packaging technology are reducing manufacturing cost, so that the price of the modules competes favorably with other energy storage designs. The HTM module is sealed from the elements in a rugged, splash-proof, IP 65-compliant, aluminum chassis, and weighs less than 50kg [3].

As well as braking recuperation, energy storage can also be used to help meet peak power demands. Ultra-capacitors offer up to 10 times the power of batteries and in terms of acceleration of a vehicle, this plays an important role [3].

2.6.2. Ultra-capacitor modeling

With this background, in this section, the detail of ultra-capacitor modeling is described. The open-circuit voltage of the ultra-capacitor is given by:

$$V_{oc} = \frac{q_{uc}}{C_{uc}} \tag{10}$$

where q_{uc} and C_{uc} are the ratio of charge and capacitance respectively. The charge dynamics of the ultra-capacitor are given by:

$$\frac{dq_{uc}}{dt} = -i_{uc} \tag{11}$$

where i_{uc} is the current being drown. Positive and negative current correspond to discharging and charging, respectively. The state-of-charge is a normalized parameter representing the amount of charge remaining in the ultra-capacitor, defined as:

$$SOC = \frac{V_{oc}}{V_{\max}} \tag{12}$$

where $V_{\max}$ is the maximum open-circuit voltage and SOC denotes state of charge. The effective voltage provided by the ultra-capacitor is:

$$V_{out} = V_{oc} - i_{uc} R_{uc}$$
$$R_{uc} = \begin{cases} R_{dis} & i_{uc} > 0 \\ R_{chg} & i_{uc} < 0 \end{cases} \tag{13}$$

R_{chg} and R_{dis} are the line resistances for charging and discharging, respectively. The two resistances are assumed to be the same, as is typically the case in an ultra-capacitor [6]. In Figure 12, the ultra-capacitor resistance by ESR is presented.

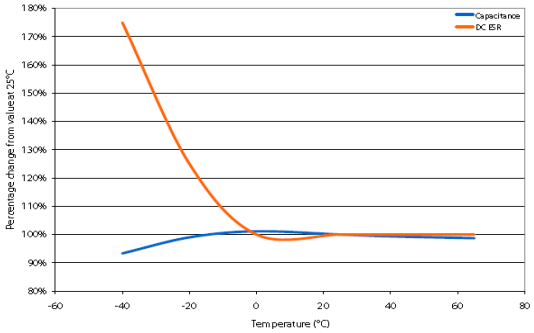

Figure 12. ESR and capacitance versus temperature of an ultra-capacitor

The current drawn from the ultra-capacitor is determined from the power P_{uc} demanded by motor, using the simple relation:

$$i_{uc} = \frac{P_{uc}}{V_{out}} \tag{14}$$

This power is bounded by the line losses in the ultra-capacitor. The maximum charging and discharging power which capacitor can support are given as [4]:

$$P_{\max,dis} = \frac{V_{oc}^2}{4R_{uc}} \tag{15}$$

$$P_{\max,chg} = V_{oc} \frac{V_{oc} - V_{\max}}{R_{uc}} \tag{16}$$

So, i_{uc} can be computed by solving the Equations (12)-(17) as:

$$i_{uc} = \frac{-SOC \cdot V_{\max} + \sqrt{(SOC \cdot V_{\max})^2 - 4R_{uc}P_{required}}}{2R_{uc}} \quad (17)$$

Based on the Maxwell information (Figure) there is not much deference in ESR and capacitance of ultra-capacitor in temperatures above 0°C, and based on the Tehran metro information, the temperature in tunnels do not fall behind this value. On the other hand, based on information discussed before, there is only a 3°C temperature rise above ambient temperature at the maximum continuous current. So, in case of simplicity the thermal dynamic of the ultra-capacitor can be ignored [24]. As illustrated in Figure, the required motor power is input of ultra-capacitor block and by the value of required power the corresponding available current of ultra-capacitor based on the available state of charge will be calculated as in Equation (17). After that the next state of charge (SOC) can be calculated and so on. This procedure will be continued until the SOC reaches its minimum or maximum value. Whenever the available power of ultra-capacitor is different with required power, the power should be provided by the supply network – here the third rail – or should be wasted by resistances. Equations (12) to (17) are used to model the ultra-capacitor as it is shown in Figure 13.

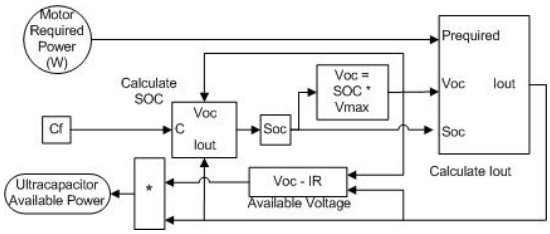

Figure 13. Ultra-capacitor model block diagram

As a test of ultra-capacitor model, a sinusoidal waveform as required power is applied to the presented model of the ultra-capacitor. The results are shown in Figure 14. The top part of the figure shows the hypothetical input power; the middle part shows the available power of the ultra-capacitor regard to the required power. The final part shows state of charge of the ultra-capacitor that should be maintained between 1 and 0.5.

These waveforms show a valid simulation of the ultra-capacitor and SOC varies between 0.5 and 1 since the state of charge of the ultra-capacitor cannot fall below 0.5 because its output voltage V_{out} decreases dramatically and this is not allowed.

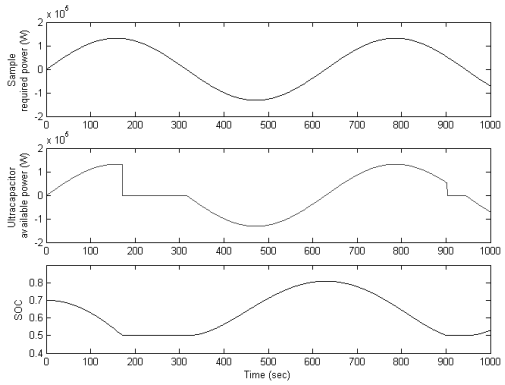

Figure 14. Ultracapacitor test waveforms

The amount of the capacitance that needs to be used in train can be calculated by Maxwell data. By considering the characteristics of the system, a power of about 150kW [24] is needed. So, there can be six modules including two series of three paralleled modules or another arrangement by six series modules. The simulations in both cases are executed. The simulation results show that the six series modules can deliver more power than the first arrangement. Because the ultra-capacitor power potential increases with the square of voltage, and only linearly decreases with resistance. This means that to increase the pack's discharge power capability, it is much better to string more cells together in series to give a higher operating voltage than to simply add strings in parallel.

2.6.3. Powerbus Modeling

Power-bus represents a simple control algorithm to choose a power source between the third rail and the ultra-capacitor. Simply by four simple if-then commands as in Equation (18) the bus can be modeled, Figure 15.

$$\begin{cases} \text{if SOC} < 0.5 \;\&\; P_{required} > 0 \;\Rightarrow\; P_{Net} = P_{required} \\ \text{if SOC} < 0.5 \;\&\; P_{required} < 0 \;\Rightarrow\; P_{Net} = 0 \\ \text{if SOC} > 0.5 \;\&\; P_{required} > 0 \;\Rightarrow\; P_{Net} = 0 \\ \text{if SOC} > 0.5 \;\&\; P_{required} < 0 \;\Rightarrow\; P_{Net} = 0 \end{cases} \quad (18)$$

This says that when the state of charge is less than 0.5 and the required power ($P_{required}$) is positive the required power should be supplied by the network (P_{Net}) and when the required power is negative there is no need to the network

since the power is used to recharge the ultra-capacitor and if it reaches its maximum charge the power is wasted by resistances. In a same way if state of charge is bigger than 0.5 there is no need to the network since if the required power is positive the ultra-capacitor supplies it and when it is negative again it charges the ultra-capacitor.

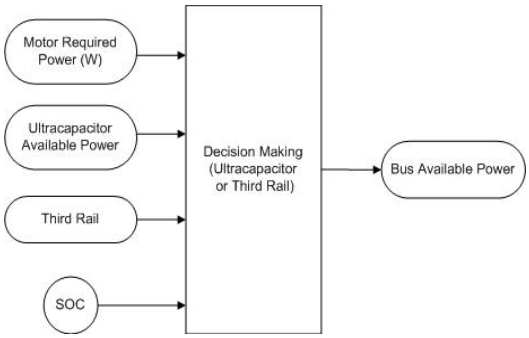

Figure 15. Bus and power control

3. Simulation Results

Simulation executed under a 5-station drive cycle and grade and curve profiles of line 2 in Tehran metro, as presented in Figure 16. It is considered that the maximum speed of the corresponding track is up to 70 Km/h.

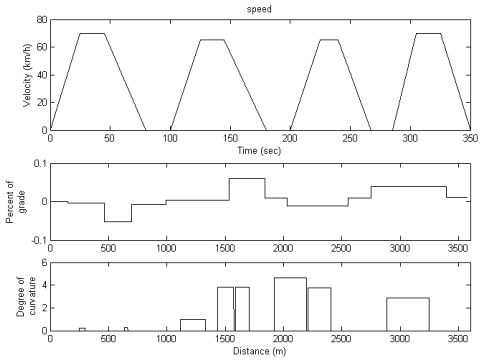

Figure 16. Desired velocity and curve and grade profile

The power characteristics are shown in Figure 17. The solid line shows the whole power that the train requires and the dashed line is the amount of the power that the ultra-capacitor covered. In negative parts of power the ultra-capacitor recharges and in the positive parts it supplies power till SOC reaches its minimum limit. Also, the ultra-capacitor characteristic is shown in Figure 18. As it is shown in Figures 17&18, with consideration of the initial SOC equal to 0.7, the ultra-capacitor can deliver more than 35% of energy required and absorbs most of braking energy. As another test, the initial SOC is 0.8, but the route profile is similar to the previous test. The results are shown in Figure 19. Obviously here, the ultra-capacitor can deliver more power. This time the percentage power delivered by the ultra-capacitor is up to 42% and it represents a very good capability of the system.

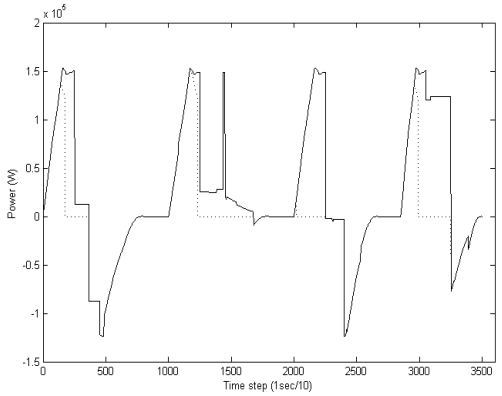

Figure 17. Power characteristic of system

(Solid line: whole required power; Dashed line: Ultra-capacitor covered power)

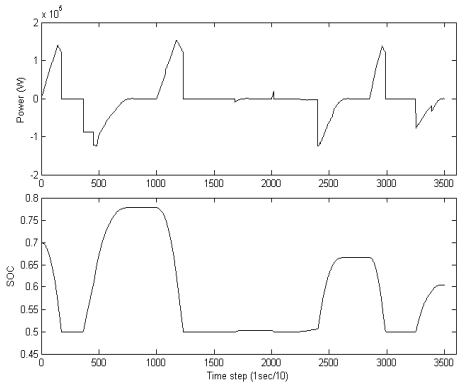

Figure 18. Ultracapacitor characteristics

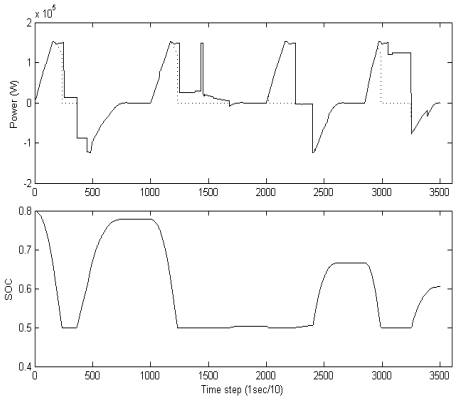

Figure 19. Characteristics of the second test with the initial SOC = 0.8

4. Conclusions

A simple and precise model of a hybrid electric train that is equipped with Maxwell 125V heavy transportation modules is modeled and simulated. The simulation results show that using the ultra-capacitors in heavy transportation like trains have benefits as in reducing the energy consumption and to prevent lack of voltage in case of voltage drops in peak hours. Using the ultra-capacitors also prevents the delay and standing still. Although it seems it that the costs are too much to equip a train with the ultra-capacitor modules but if it is considered, up to 40 percent of reducing energy for fifteen years for a large system like the undergrounds is possible.

List of symbols

A	cross sectional area of vehicle	m^2
a	Acceleration	m/s^2
B	Coefficient of Moving Friction	-
C	Air Resistant Coefficient	-
C_{uc}	Ultra-capacitor Capacity	F
F	Force	N
F_T	Tractive Force	N
G	Percentage of Grade	%
G_{FB}	Gear Ratio	-
i_{uc}	Ultra-capacitor Current	A
J	Wheel Inertia	$Kg \cdot m^2$
m	Weight per Axle	Kg
n	Number of Axles	-
P_{uc}	Ultra-capacitor Power	$Watt$
q_{uc}	Ultra-capacitor ratio of charge	coulombs
r	Wheel Radius	m
R_C	Curve Resistance	N
R_D	Resistance Forces	N
R_g	Grade Resistance	N
R_{uc}	Ultra-capacitor Resistance	Ω
S_x	Longitudinal Slip	-
SOC	State of Charge	-
T	Torque	$N \cdot m$
V_{oc}	Ultra-capacitor Open Circuit Voltage	$volt$
V_{max}	Ultra-capacitor Maximum Voltage	$volt$
V_{min}	Ultra-capacitor Minimum Voltage	$volt$

Greek symbols

v	Linear Speed	m/s
ω	Angular Velocity	rad/s

References

[1] S. Matsumoto, Advancement of hybrid vehicle technology, European Conference on Power Electronics and Applications, (Sept. 2005), Dresden, Germany.

[2] E. LO, Review on the Configurations of Hybrid Electric Vehicles, 3rd International Conference on Power Electronics Systems and Applications, (May 2009).

[3] A. Schneuwly, Energy storage for hybrid power in heavy, White paper, http://www.maxwell.com.

[4] S.A. Schepmann, Ultracapacitor heavy hybrid vehicle: model predictive control using future information to improve fuel consumption, Master of Science Mechanical Engineering thesis, Clemson University, 2010.

[5] Adrian Schneuwly, Rail Power, White paper, http://www.maxwell.com.

[6] D. Rotenberg, Ultracapacitor assisted power trains: Modeling, control, and sizing the impact on fuel economy, Master of Science Mechanical Engineering thesis, Clemson University, 2008.

[7] D.W. Gao, C. Mi, A. Emadi, Modeling and simulation of electric and hybrid vehicles, Proceedings of the IEEE, Vol. 95, No. 4, (April 2007), pp.729-745.

[8] A. Khaligh, Z. Li, Battery, Ultracapacitor, fuel cell, and hybrid energy storage systems for electric, hybrid electric, fuel cell, and plug-in hybrid electric vehicles: State of the Art, IEEE Transactions on Control Systems Technology, Vol. 59, No. 6, (2010), pp.2806-2814.

[9] J. Liu, H. Pen, Modeling and control of a power-split hybrid vehicle, IEEE Transactions on Control Systems Technology, Vol. 16, No. 6, (2008), pp.1242-1251.

[10] D. Hong, H. Lee, J. Kwak, Development of a mathematical model of a train in the energy point of view, International Conference on Control, Automation and Systems (2007), pp.350-355.

[11] MITRAC Datasheet, http://www.bombardier.com.

[12] S. Zoroofi, Modeling and simulation of vehicular power systems, Master's thesis in Power Engineering, Department of Energy and Environment Division of Electric Power Engineering Chalmers University of Technology, Goteborg, Sweden, (2008).

[13] A. Hipp, Track and signal plan, Tehran Metro Line 2, E2 To X2, Tehran Metro Archive, Released 2005.

[14] Z. Rahman, K. Bulter, M. Ehsani, Designing parallel hybrid -electric vehicle using V-ELPH, Proceedings of American Control Conference, (1999), pp.2693-2697.

[15] K.B. Wipke, M.R. Cuddy, and Steven D. Burch, ADVISOR 2.1: A user-friendly advanced powertrain simulation using a combined backward/forward approach, IEEE Transactions on Vehicular Technology, Vol. 48, No. 6, (1999), pp.1751-1761.

[16] T. Markel, A. Brooker, T. Hendricks, V. Johnson, K. Kelly, B. Kramer, M. O'Keefe, S. Sprik, K. Wipke, ADVISOR: a systems analysis tool for advanced vehicle modeling, Journal of Power Sources 110, (2002), pp.255-266.

[17] R. Von Hanxleden, Model-based design and distributed real-time systems, Christian-Albrechts Universit¨at Kiel, (2006).

[18] A.J. Horowitz, The vehicle – propulsion and resistance, Internal university paper, University of Wisconsin – Milwaukee, (2000).

[19] S. Iwnicki, Handbook of Railway Vehicle Dynamics, CRC Press Taylor & Francis Group, (2006).

[20] J.B. Calvert, Degree of curvature, Railways: History, Signaling, Engineering, (2004).

[21] G. Rill1, Wheel dynamics, Proceedings of the XII International Symposium on Dynamic Problems of Mechanics, ABCM, Ilhabela, SP, Brazil, (2007).

[22] S.M. Lukic and A. Emadi, Modeling of electric machines for automotive applications using efficiency maps, Illinois Institute of Technology, Proceedings of the IEEE, (2003).

[23] S. Williamson, A. Emadi, K. Rajashekara, Comprehensive efficiency modeling of electric traction motor drives for hybrid electric vehicle propulsion applications, IEEE Transactions on Vehicular Technology, Vol. 56, No. 4, (2007), pp.1561-1572.

[24] Datasheet 125V Heavy transportation modules, http://www.maxwell.com